Maximum Likelihood Alamouti Receiver for Filter Bank Based Multicarrier Transmissions

Pascal Chevalier*†, Didier Le Ruyet*, Rémi Chauvat*†
*CNAM, CEDRIC Laboratory, 292 rue Saint-Martin, 75003 Paris, France
†Thales-Communications-Security, HTE/AMS/TCP, 4 Av. des Louvresses, 92622 Gennevilliers, France

***Abstract*—Filter-bank based multicarrier (FBMC) transmission is an alternative to orthogonal frequency division multiplexing (OFDM) transmission, more spectrally efficient and more robust to asynchronisms than the latter. For these reasons, the FBMC waveform is a promising candidate for 5G mobile networks. Using offset quadrature amplitude (OQAM) symbols and a proper prototype filter, the FBMC waveform may become orthogonal for flat fading single-input single-output (SISO) channels. However, for frequency selective or multiple-input multiple-output (MIMO) channels, the FBMC waveform is generally no longer orthogonal and inter-carrier interference (ICI) is present at reception. This ICI makes difficult the combination of FBMC waveforms with some MIMO schemes such as the Alamouti scheme in particular. In this context, the purpose of this paper is to introduce a new Alamouti receiver for the detection of the OQAM symbols transmitted by a FBMC waveform. This receiver is based on the maximum likelihood (ML) joint detection of the symbols transmitted by both the subcarrier of interest and its two adjacent subcarriers. Challenges for the receiver implementation are discussed jointly with sub-optimal alternatives to decrease the complexity.**

I. Introduction

FBMC waveforms are an alternative to OFDM waveforms, much better localized in the frequency domain and offering a better spectral efficiency than the latter. Moreover, FBMC waveforms do not require any cyclic prefix (CP) and are more robust to asynchronisms than OFDM waveforms [1]. For these reasons, FBMC waveforms are a promising candidate for 5G mobile networks [2]. It has been shown in [3] that by using OQAM constellations, it is possible to achieve a baud-rate spacing between adjacent subcarriers and still recover the information symbol, free of both inter-symbol interference (ISI) and ICI, for ideal or flat fading SISO propagation channels. This gives rise to FBMC-OQAM waveforms whose efficient implementations based on the discrete Fourier transform are given in [4], [5]. However, for frequency selective or MIMO propagation channels, the FBMC waveform loses its orthogonal character and ICI is present at reception.

In recent years, FBMC waveforms have attracted a lot of interest and many equalization and synchronization methods have been proposed for SISO systems corrupted by frequency selective propagation channels [6–8]. However, if multiple antennas are incorporated at both ends of the link, MIMO communications can be designed to boost the performance, in terms of reliability or bit rate, as shown in [9], [10]. Nevertheless, due to the presence of ICI at reception, the way to reach the full potential of MIMO schemes for FBMC waveforms remains an open topic.

Recently, some transmitter-receiver designs using channel state information (CSI) at transmission have been proposed for MIMO FBMC-OQAM systems for both single-user [11], [12] and multi-user transmissions [13–18]. Several receiver designs have also been developed for MIMO FBMC-OQAM systems exploiting no CSI at transmission and using spatial multiplexing [19–24].

The works related to MIMO FBMC-OQAM systems using space-time coding mainly concern the Alamouti scheme [25]. Note that the latter is a space-time block code aiming at extracting the full spatial diversity of the system at transmission. Despite the fact that FBMC system is not a block transmission system due to ISI, the Alamouti scheme may still be used to extract the spatial diversity of the system at transmission provided the ISI is efficiently processed by the receiver, as shown in [26] in another context. However, due to the presence of ICI at reception, the Alamouti scheme, which can be implemented easily for OFDM transmissions, cannot be directly applied to FBMC-OQAM waveforms [27]. For this reason, several transmitter-receiver designs have been proposed recently to couple the Alamouti scheme with FBMC-OQAM waveforms. Unfortunately, all these solutions have serious drawbacks. In particular, a pseudo-Alamouti transceiver is proposed in [27] for FBMC-OQAM systems, whereas a new FBMC scheme, called FFT-FBMC, allowing to easily couple the Alamouti scheme with FBMC-OQAM waveforms is proposed in [23], but both solutions require the insertion of a CP. A block-wise version of the Alamouti scheme for FBMC-OQAM systems is proposed in [28] but it requires the insertion of guardbands and guard periods between the blocks, which decreases the spectral efficiency. In [29] it is shown that the Alamouti scheme can be coupled with FBMC-OQAM waveforms but provided that it is combined with code division multiple access (CDMA). In [30] a modification of the Alamouti scheme is proposed for FBMC-OQAM waveforms, jointly with an iterative processing at reception to cancel ICI. However, this iterative processing may generate error propagation for moderate signal to noise ratio.

In this context, the purpose of this paper is to introduce a new Alamouti receiver for FBMC-OQAM waveforms. For each subcarrier, this receiver is based on the ML joint detection of the symbols transmitted by the subcarrier of interest and its two adjacent subcarriers, assuming that the adjacent subcarriers are the only ones which contribute to the ICI. Challenges for the receiver implementation are discussed jointly with sub-optimal alternatives to decrease the complexity. The proposed receiver does not have the drawbacks of existing solutions but requires the ML joint detection of three subcarriers per subcarrier, which may be costly for constellations with high number of states.

The system model associated with the Alamouti scheme for a FBMC-OQAM waveform is introduced in section II. The proposed ML Alamouti receiver is presented in section III, together with its main properties, implementation issues and associated complexity. Section IV concludes the paper.

II. Reception model

A. Transmitted Alamouti FBMC-OQAM signals

Let us recall that the baseband signal, $s(t)$, of an OQAM signal transmitting the complex symbols c_k, of duration T_s, can be written as

$$s(t) = \sum_k c_k^r v(t - kT_s) + j c_k^i v(t - kT_s - T_s/2) \qquad (1)$$

where c_k^r and c_k^i are real quantities corresponding to the real part and the imaginary part of the associated QAM symbol c_k respectively, whereas $v(t)$ is the pulse shaping filter. Defining the real symbols b_{2k} and b_{2k+1} by $b_{2k} \triangleq (-1)^k c_k^r$ and $b_{2k+1} \triangleq (-1)^k c_k^i$ respectively, it is straightforward to show that $s(t)$ can also be written as

$$s(t) = \sum_k j^k b_k v(t - kT) \triangleq \sum_k a_k v(t - kT) \qquad (2)$$

where $T \triangleq T_s/2$ and $a_k \triangleq j^k b_k$. Equation (2) means that the OQAM signal (1) can also be interpreted as a signal which transmits, without any staggering operation, the complex symbols a_k, or the real symbols b_k, with a symbol duration equal to T.

We consider a radio communication system that employs the Alamouti scheme, with two transmit antennas [25], on each subcarrier of a FBMC-OQAM waveform, as depicted at Fig. 1. Under this assumption and using (2), the baseband signals, $s_1(t)$ and $s_2(t)$, transmitted by antennas 1 and 2 respectively, can be written as

$$s_1(t) = \sum_{l=0}^{L-1} \sum_k \left[a_{l,2k-1} v(t-(2k-1)T) - a_{l,2k}^* v(t-2kT)\right] j^l e^{j\pi \frac{lt}{T}} \qquad (3)$$

$$s_2(t) = \sum_{l=0}^{L-1} \sum_k \left[a_{l,2k} v(t-(2k-1)T) + a_{l,2k-1}^* v(t-2kT)\right] j^l e^{j\pi \frac{lt}{T}} \qquad (4)$$

Here, $(.)^*$ means complex conjugate, L is the number of subcarriers, $1/2T = 1/T_s$ is the subcarrier spacing, $v(t)$ is the prototype filter and $a_{l,k} \triangleq j^k b_{l,k}$, where $b_{l,k}$ is the real symbol transmitted (without the Alamouti encoding) at time kT on subcarrier l. Note that the Alamouti scheme is applied here to the complex symbols $a_{l,k} = j^k b_{l,k}$ (which are either real or purely imaginary) of duration $T = T_s/2$, and not to the associated QAM symbols, $c_{l,k} \triangleq (-1)^k [b_{l,2k} + j b_{l,2k+1}]$ of duration T_s, before staggering. This allows to consider spatio-temporal Alamouti code words of duration T_s instead of $2T_s$ and this imposes constant propagation channels over T_s instead of $2T_s$. Note that the Alamouti scheme has already been applied with success to real-valued symbols instead of complex ones in [31].

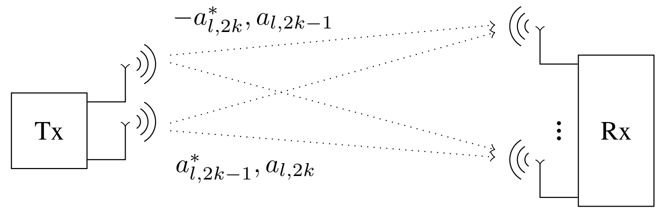

Fig. 1. MIMO $2 \times N$ system using Alamouti space-time coding per subcarrier

B. Received Alamouti FBMC-OQAM signals

Assuming a reception with N antennas, and denoting by $\mathbf{h}_i(t)$ $(i = 1, 2)$ the impulse response vector of the propagation channel between the transmit antenna i and the reception array, the observation vector at time t at the output of the receive antennas is given by

$$\mathbf{x}(t) = \sum_{i=1}^{2} s_i(t) * \mathbf{h}_i(t) + \mathbf{n}(t) \qquad (5)$$

Here, $*$ is the convolution operation, $\mathbf{n}(t)$ is the background noise vector assumed to be zero-mean, Gaussian, circular, stationary, spatially and temporally white.

C. Observation model after low-pass filtering

Considering that l_0 is the subcarrier of interest for the processing we consider, the vector $\mathbf{x}(t)$ is first frequency shifted by $e^{-j\pi l_0 t/T}$ to put the subcarrier l_0 at baseband. Then an arbitrary low-pass filter, $p(t)$, is applied to the shifted observation vector to isolate the baseband contribution of the subcarrier l_0 and to remove both the noise outside its bandwidth and the subcarriers which do not overlap with l_0. The bandwidth B of the filter $p(t)$ must be that of a subcarrier, i.e. $B = 2/T_s = 1/T$. An example of filter $p(t)$ may be $v^*(-t)$, the matched filter associated with $v(t)$, but this is not mandatory. Under these assumptions, we deduce from (5) that the observation vector after frequency shifting and low-pass filtering takes the form

$$\begin{aligned}
\mathbf{x}_p(t) &\triangleq p(t) * \left[e^{-j\pi \frac{l_0 t}{T}} \mathbf{x}(t)\right] \\
&= \sum_{i=1}^{2} p(t) * \left[e^{-j\pi \frac{l_0 t}{T}} s_i(t) * \mathbf{h}_i(t)\right] + \mathbf{n}_p(t) \\
&\triangleq \sum_{i=1}^{2} \mathbf{s}_{ph,i}(t) + \mathbf{n}_p(t) \qquad (6)
\end{aligned}$$

Here, $\mathbf{n}_p(t) \triangleq p(t) * [e^{-j\pi l_0 t/T} \mathbf{n}(t)]$ and $\mathbf{s}_{ph,i}(t) \triangleq p(t) * [e^{-j\pi l_0 t/T} s_i(t) * \mathbf{h}_i(t)]$.

III. Maximum Likelihood receiver

A. Presentation of the ML approach

The receiver which is proposed in this paper consists first in jointly demodulating, from a ML approach, the subcarrier of interest, l_0, and the subcarriers which overlap with the latter after the low-pass filtering operation. Then, the idea is to retain only the demodulated symbols belonging to the subcarrier of interest, l_0, and to discard the others. The operation of joint demodulation of the overlapped subcarriers aims at mitigating the ICI for the subcarrier l_0 instead of considering ICI as an additional noise for l_0. The subcarriers corresponding to the ICI for the subcarrier l_0 are then discarded since they will be much better demodulated when they will correspond themselves to the subcarrier of interest.

In order to take easily into account the potential temporal coloration property of $\mathbf{n}_p(t)$ and to remove the potential influence of the sampling rate, we adopt a continuous time ML approach to develop the proposed receiver. In this context, under the assumptions of section II-B, we deduce from (6) that the ML joint detection of the symbols belonging to the subcarrier of interest l_0 and to the $2M$ subcarriers which overlap with the latter, consists in generating the symbol set $\mathbf{b} = \{b_{l,k}, l_0 - M \leq l \leq l_0 + M, k \in Z\}$ which minimizes the following criterion [32], [33][1]

$$\mathrm{C}(\mathbf{b}) = \int_B \left[\mathbf{x}_p(f) - \sum_{i=1}^{2} \mathbf{s}_{ph,i}(f)\right]^H \mathbf{R}_{n,p}^{-1}(f) \left[\mathbf{x}_p(f) - \sum_{i=1}^{2} \mathbf{s}_{ph,i}(f)\right] df \tag{7}$$

where $(.)^H$ means transpose and conjugate whereas $\mathbf{R}_{n,p}(f)$ is the power spectral density matrix of $\mathbf{n}_p(t)$, defined by

$$\mathbf{R}_{n,p}(f) = N_0 \left|p(f)\right|^2 \mathbf{I} \tag{8}$$

where N_0 is the power spectral density of $\mathbf{n}(t)$ and $\mathbf{I}$ is the identity matrix. We assume in the following that the propagation channels are known and approximately flat over the bandwidth B. This holds in practice as long as the delay spread of the channels remains much lower than T, which is always true beyond a sufficient number of subcarriers. Under this assumption, we deduce from (6) that $\mathbf{s}_{ph,i}(f)$ can be written as

$$\mathbf{s}_{ph,i}(f) = p(f) s_i\Big(f + \frac{l_0}{2T}\Big)\mathbf{h}_i = p(f) s_{R,i}\Big(f + \frac{l_0}{2T}\Big)\mathbf{h}_i \tag{9}$$

where $\mathbf{h}_i \triangleq \mathbf{h}_i(f + l_0/2T) = \mathbf{h}_i(l_0/2T)$ and $s_{R,i}(f + l_0/2T) \triangleq s_i(f + l_0/2T) R_B(f)$, $(i = 1, 2)$, such that $R_B(f) = 1$ for $-B/2 \leq f \leq B/2$ and $R_B(f) = 0$ otherwise. Moreover, we assume that $M = 1$, i.e. that only the two adjacent subcarriers, $l_0 - 1$ and $l_0 + 1$, overlap with the subcarrier l_0. Note that this assumption is in particular true for the PHYDYAS prototype filter [34] which is chosen for this paper. Besides, to simplify the notations, we denote by $b_{m,k}$ the real-valued symbol $b_{l_0+m,k}$ $(-1 \leq m \leq 1)$ and we consider that $a_{m,k} \triangleq j^k b_{m,k}$. Under these assumptions, we deduce from (3) and (4) that

$$s_{R,1}\Big(f + \frac{l_0}{2T}\Big) = R_B(f) \sum_{m=-1}^{1} \sum_k \left[a_{m,2k-1} e^{j2\pi T f}(-1)^m - a^*_{m,2k}\right] e^{-j4\pi k T f} v\Big(f - \frac{m}{2T}\Big) j^{l_0+m} \tag{10}$$

$$s_{R,2}\Big(f + \frac{l_0}{2T}\Big) = R_B(f) \sum_{m=-1}^{1} \sum_k \left[a_{m,2k} e^{j2\pi T f}(-1)^m + a^*_{m,2k-1}\right] e^{-j4\pi k T f} v\Big(f - \frac{m}{2T}\Big) j^{l_0+m} \tag{11}$$

Using (8) and (9) into (7), we obtain an alternative expression of (7) given by

$$\mathrm{C}(\mathbf{b}) = \frac{1}{N_0} \int \left\| \mathbf{x}_R(f) - \sum_{i=1}^{2} s_{R,i}\Big(f + \frac{l_0}{2T}\Big)\mathbf{h}_i \right\|^2 df \tag{12}$$

where $\mathbf{x}_R(f) \triangleq R_B(f)\mathbf{x}(f + l_0/2T)$. Criterion (12) shows that the joint ML receiver depends on the prototype filter $v(t)$ but does not depend on the form of the low-pass filter $p(t)$, provided that $p(f) \neq 0$ for $-B/2 \leq f \leq B/2$. Inserting (10) and (11) into (12), we obtain, after straightforward manipulations

$$\mathrm{C}(\mathbf{b}) = \frac{1}{N_0} \int \Bigg\| \mathbf{x}_R(f) - R_B(f) \sum_{m=-1}^{1} \sum_k e^{-j4\pi k T f} v\Big(f - \frac{m}{2T}\Big) \times j^{l_0+m}(-1)^k \Big\{ j b_{m,2k-1}\left[e^{j2\pi T f}(-1)^{m+1}\mathbf{h}_1 + \mathbf{h}_2\right] + b_{m,2k}\left[e^{j2\pi T f}(-1)^m \mathbf{h}_2 - \mathbf{h}_1\right] \Big\} \Bigg\|^2 df \tag{13}$$

B. Alternative expression of $\mathrm{C}(\mathbf{b})$

To express the criterion $\mathrm{C}(\mathbf{b})$ as a function of discrete-time signals only, we must introduce a set of quantities defined hereafter. We introduce the following quantities: $v_m(t) \triangleq v(t)e^{j\pi m t/T}$, $\mathbf{x}_{Rv,m}(t) \triangleq e^{-j\pi l_0 t/T}\mathbf{x}(t) * R_B(t) * v_m^*(-t)$, $r_m(t) \triangleq v^*(-t) * v_m(t)$ and $r_{R,m,n}(t) \triangleq v_n^*(-t) * R_B(t) * v_m(t)$, for $(-1 \leq m, n \leq 1)$, where we recall that $R_B(t)$ is the inverse Fourier transform of $R_B(f)$. The quantities $\mathbf{x}_{Rv,m}(t)$ and $r_{R,m,n}(t)$ are the inverse Fourier Transform of their Fourier Transform and we then obtain

$$\mathbf{x}_{Rv,m}(t) = \int e^{j2\pi f t}\mathbf{x}_R(f) v^*\Big(f - \frac{m}{2T}\Big) df \tag{14}$$

$$r_{R,m,n}(t) = \int e^{j2\pi f t} R_B(f) v^*\Big(f - \frac{n}{2T}\Big) v\Big(f - \frac{m}{2T}\Big) df \tag{15}$$

Note that the samples $r_m(kT)$ for $(-1 \leq m \leq 1, -4 \leq k \leq 4)$ define the joint ISI/ICI table of the PHYDYAS prototype filter, corresponding to Table I. These samples are zero for $|k| > 4$. The samples $r_{R,m,n}(kT)$ define another ISI/ICI table related to Table I by the following relations: $r_{R,m,0}(kT) = r_m(kT)$ and $r_{R,0,n}(kT) = (-1)^{kn} r_{-n}(kT)$ for $(-1 \leq m, n \leq 1)$, $r_{R,1,-1}(kT) = r_{R,-1,1}(kT) = 0$, $r_{R,1,1}(kT) = (-1)^k I_1(kT)$

[1] All Fourier transforms of vectors $\mathbf{x}$ and matrices $\mathbf{X}$ use the same notation where t is simply replaced by f.

Carrier m \ Symbol k	-4	-3	-2	-1	0	1	2	3	4
-1	0.0054	j0.0429	-0.1250	-j0.2058	0.2393	j0.2058	-0.1250	-j0.0429	0.0054
0	0	-0.0668	0	0.5644	1	0.5644	0	-0.0668	0
1	0.0054	-j0.0429	-0.1250	j0.2058	0.2393	-j0.2058	-0.1250	j0.0429	0.0054

TABLE I
ISI/ICI TABLE OF THE PHYDYAS PROTOTYPE FILTER ($r_m(kT)$)

and $r_{R,-1,-1}(kT) = (-1)^k I_{-1}(kT)$ where $I_1(kT)$ and $I_{-1}(kT)$ are defined by

$$I_1(kT) = \int_{-\frac{1}{2T}}^{0} e^{j2\pi kTf} |v(f)|^2 \, df \tag{16}$$

$$I_{-1}(kT) = \int_{0}^{\frac{1}{2T}} e^{j2\pi kTf} |v(f)|^2 \, df \tag{17}$$

It is easy to verify that $\Re[I_1(kT)] = \Re[I_{-1}(kT)] = r_0(kT)/2$ while $\Im[I_1(kT)] = -\Im[I_{-1}(kT)]$ has an infinite support whose first values are illustrated at Fig. 2.

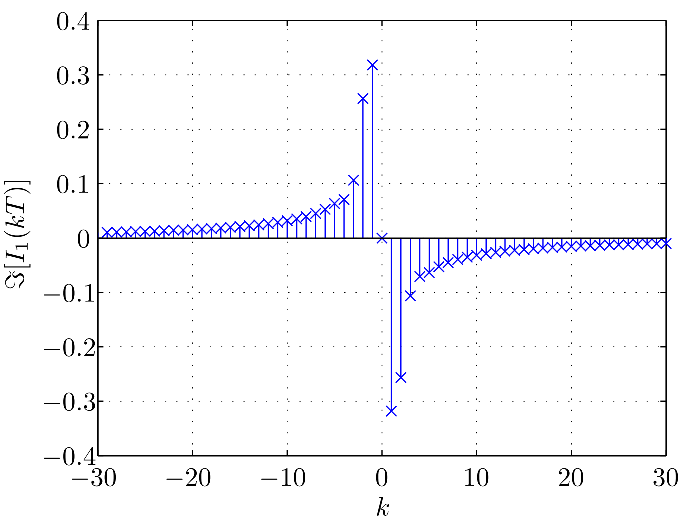

Fig. 2. $\Im[I_1(kT)]$ as a function of k

We define the (3×1) and (6×1) vectors $\mathbf{b}_k$ and $\widetilde{\mathbf{b}}_k$ by $\mathbf{b}_k \triangleq [b_{-1,k}, b_{0,k}, b_{1,k}]^T$ and $\widetilde{\mathbf{b}}_k \triangleq [\mathbf{b}_{2k-1}^T, \mathbf{b}_{2k}^T]^T$ and the $(3N \times 1)$ and $(6N \times 1)$ vectors $\widetilde{\mathbf{x}}_{Rv}(kT)$ and $\widetilde{\mathbf{x}}(kT)$ by $\widetilde{\mathbf{x}}_{Rv}(kT) \triangleq [\mathbf{x}_{Rv,-1}^T(kT), \mathbf{x}_{Rv,0}^T(kT), \mathbf{x}_{Rv,1}^T(kT)]^T$ and $\widetilde{\mathbf{x}}(kT) \triangleq [\widetilde{\mathbf{x}}_{Rv}^T((2k-1)T), \widetilde{\mathbf{x}}_{Rv}^T(2kT)]^T$. We also define the $(6 \times 6N)$ channel matrix H by

$$H \triangleq \begin{pmatrix} H_{11} & H_{12} \\ H_{21} & H_{22} \end{pmatrix} \tag{18}$$

where the $(3 \times 3N)$ matrices H_{ij} $(1 \leq i,j \leq 2)$ are defined by $H_{11} \triangleq \Lambda_{11} K_1^H$, $H_{12} \triangleq \Lambda_{11}^* K_2^H$, $H_{21} \triangleq -j\Lambda_{11} K_2^H$, $H_{22} \triangleq -j\Lambda_{11}^* K_1^H$, where the (3×3) matrix Λ_{11} is defined by $\Lambda_{11} \triangleq \mathrm{Diag}(1, j, -1)$ whereas the $(3 \times 3N)$ matrix K_i^H $(1 \leq i \leq 2)$ is defined by

$$K_i^H \triangleq \begin{pmatrix} \mathbf{h}_i^H & & \\ & \mathbf{h}_i^H & \\ & & \mathbf{h}_i^H \end{pmatrix} \tag{19}$$

Finally, we define the (6×6) matrix $F(k)$ by

$$F(k) \triangleq \begin{pmatrix} F_{11}(k) & F_{12}(k) \\ F_{21}(k) & F_{22}(k) \end{pmatrix} \tag{20}$$

where $F_{ij}(k)$ $(1 \leq i,j \leq 2)$ are (3×3) matrices whose coefficients $F_{ij}(k)[2+m, 2+n]$ for $(-1 \leq m,n \leq 1)$ are such that

$$\begin{aligned} F_{11}(k)[2+m, 2+n] \triangleq & j^{n-m} \Big\{ \Big[(-1)^{m+n} \mathbf{h}_1^H \mathbf{h}_1 + \mathbf{h}_2^H \mathbf{h}_2 \Big] \\ & \times r_{R,n,m}(2kT) + (-1)^{m+1} \mathbf{h}_1^H \mathbf{h}_2 r_{R,n,m}((2k-1)T) \\ & + (-1)^{n+1} \mathbf{h}_2^H \mathbf{h}_1 r_{R,n,m}((2k+1)T) \Big\} \end{aligned} \tag{21}$$

$$\begin{aligned} F_{12}(k)[2+m, 2+n] \triangleq & -j^{n-m+1} \Big\{ \Big[(-1)^{m+n+1} \mathbf{h}_1^H \mathbf{h}_2 - \mathbf{h}_2^H \mathbf{h}_1 \Big] \\ & \times r_{R,n,m}(2kT) + (-1)^{m} \mathbf{h}_1^H \mathbf{h}_1 r_{R,n,m}((2k-1)T) \\ & + (-1)^{n} \mathbf{h}_2^H \mathbf{h}_2 r_{R,n,m}((2k+1)T) \Big\} \end{aligned} \tag{22}$$

$$\begin{aligned} F_{21}(k)[2+m, 2+n] \triangleq & j^{n-m+1} \Big\{ \Big[(-1)^{m+n+1} \mathbf{h}_2^H \mathbf{h}_1 - \mathbf{h}_1^H \mathbf{h}_2 \Big] \\ & \times r_{R,n,m}(2kT) + (-1)^{m} \mathbf{h}_2^H \mathbf{h}_2 r_{R,n,m}((2k-1)T) \\ & + (-1)^{n} \mathbf{h}_1^H \mathbf{h}_1 r_{R,n,m}((2k+1)T) \Big\} \end{aligned} \tag{23}$$

$$\begin{aligned} F_{22}(k)[2+m, 2+n] \triangleq & j^{n-m} \Big\{ \Big[(-1)^{m+n} \mathbf{h}_2^H \mathbf{h}_2 + \mathbf{h}_1^H \mathbf{h}_1 \Big] \\ & \times r_{R,n,m}(2kT) + (-1)^{m+1} \mathbf{h}_2^H \mathbf{h}_1 r_{R,n,m}((2k-1)T) \\ & + (-1)^{n+1} \mathbf{h}_1^H \mathbf{h}_2 r_{R,n,m}((2k+1)T) \Big\} \end{aligned} \tag{24}$$

Using these notations and inserting (14) and (15) into (13), we obtain an alternative expression of $\mathrm{C}(\mathbf{b})$, given by

$$\begin{aligned} \mathrm{C}(\mathbf{b}) = & \frac{1}{N_0} \Big\{ -2 \sum_k (-1)^k \widetilde{\mathbf{b}}_k^T \Re\Big[j^{-l_0} H \widetilde{\mathbf{x}}(kT) \Big] \\ & + \sum_k \sum_i (-1)^{k+i} \widetilde{\mathbf{b}}_k^T F(k-i) \widetilde{\mathbf{b}}_i \Big\} \end{aligned} \tag{25}$$

Using (20) and the definition of $\widetilde{\mathbf{b}}_k$, (25) can also be written as

$$\begin{aligned} \mathrm{C}(\mathbf{b}) = & \frac{1}{N_0} \Big\{ -2 \sum_k (-1)^k \widetilde{\mathbf{b}}_k^T \Re\Big[j^{-l_0} H \widetilde{\mathbf{x}}(kT) \Big] \\ & + \sum_k \sum_i (-1)^{k+i} \Big\{ \mathbf{b}_{2k-1}^T F_{11}(k-i) \mathbf{b}_{2i-1} \\ & + \mathbf{b}_{2k}^T F_{22}(k-i) \mathbf{b}_{2i} + \mathbf{b}_{2k-1}^T \big[F_{12}(k-i) \\ & + F_{21}^T(i-k) \big] \mathbf{b}_{2i} \Big\} \Big\} \end{aligned} \tag{26}$$

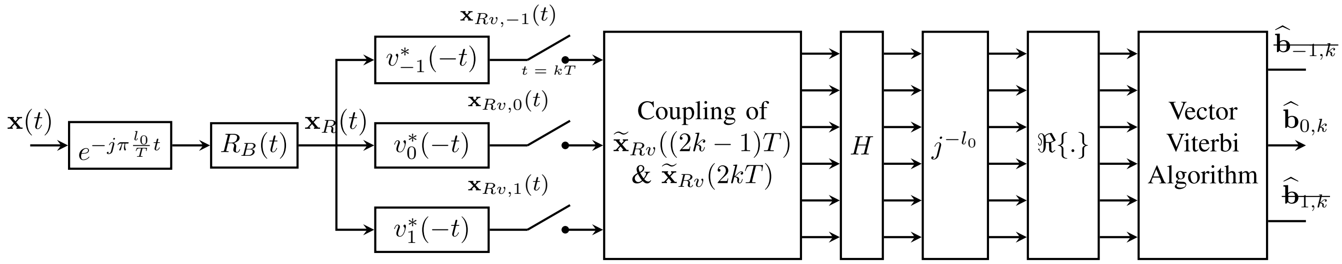

Fig. 3. Structure of the ML receiver for l_0

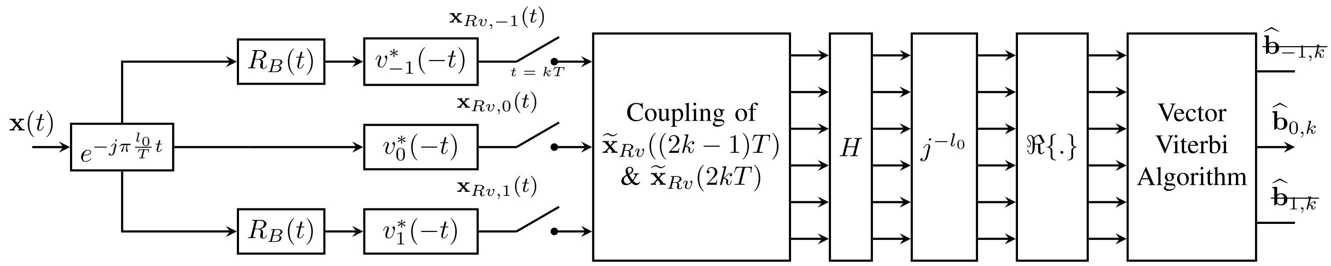

Fig. 4. Alternative structure of the ML receiver for l_0

Using (16), (17), Table I and (21) to (24), it is possible to verify that the (3×3) coupling matrix, $K_{12}[k] \triangleq F_{12}(k)+F_{21}^T(-k)$, between the symbol vectors at odd and even sample times is not zero. More precisely, it can be verified that $K_{12}(k)$ has only two non-zero elements corresponding to $K_{12}(k)[1,1]$ and $K_{12}(k)[3,3]$, which are associated with the couples $(m,n) = (-1,-1)$ and $(m,n) = (1,1)$ respectively. We deduce from this result that the two sets of symbol vectors $\{\mathbf{b}_{2k-1}\}$ and $\{\mathbf{b}_{2k}\}$ cannot be demodulated separately but have to be jointly demodulated. The problem is then to find the set of symbol vectors, $\widetilde{\mathbf{b}}_k$, which minimizes (25).

C. Interpretation

The vector $\widetilde{\mathbf{x}}(kT)$ appearing in (25) contains the samples, at odd and even sample times, $(2k-1)T$ and $2kT$, of the vectors $\mathbf{x}_{Rv,m}(t)$ for $(-1 \leq m \leq 1)$. Moreover, expression (14) shows that $\mathbf{x}_{Rv,m}(kT)$ is the sample, at time kT, of the output of the matched filter, $v_m^*(-t)$, whose input is $\mathbf{x}_R(t) \triangleq R_B(t) * (e^{-j\pi l_0 t/T}\mathbf{x}(t))$. The structure of the ML receiver for the subcarrier of interest l_0 is depicted at Fig. 3. It is composed of a frequency shifting operation which puts the subcarrier l_0 at baseband, a low-pass filtering by the ideal filter $R_B(t)$, which keeps the subcarrier l_0, removes the subcarriers which do not overlap with l_0 and keeps a temporally white noise inside its bandwidth, a set of three filters, $v_m^*(-t)$ $(-1 \leq m \leq 1)$, adapted to the pulse shaping filter of each of the three subcarriers we jointly demodulate, a sampling operation at the symbol rate T, a coupling of the samples of the matched filters outputs at odd and even time samples, a matched filtering operation to the propagation channels, a derotation operation of the subcarrier l_0, a real part capture, a decision box implementing the vector Viterbi algorithm and a box which keeps only the decided symbols of the subcarrier of interest. Using the fact that $R_B(t)*v_0^*(-t) = R_B(t)*v^*(-t) = v^*(-t)$, an equivalent structure of the ML receiver is presented at Figure 4, where the filter $R_B(t)$ has been removed from the branch associated with the subcarrier $m = 0$.

D. Implementation issues and perspectives

Once the propagation channels vectors, $\mathbf{h}_i$ $(i = 1,2)$, have been estimated, the first difficulty which is encountered to implement the previous ML receiver is related to the fact that $R_B(t)$ is a non-causal infinite impulse response, impossible to implement. The second difficulty, which is related to the first one, concerns the size of the ISI before decision, which controls the complexity of the vector Viterbi algorithm and which is infinite, as shown by Fig. 2, due to the presence of the ideal low-pass filter $R_B(t)$.

In practice, the first difficulty may be solved by replacing in Fig. 3 or Fig. 4, the filter $R_B(t)$ by an arbitrary low-pass filter $p(t)$, having a bandwidth B, and whose time support is as small as possible to minimize the size of the ISI before decision. One solution may be to choose $p(t) = v^*(-t)$, the filter matched to the PHYDYAS prototype filter. Once this choice has been done, the structures of Fig. 3 or Fig. 4 may be modified accordingly, by replacing in all parts of these structures, the parameters which are built from the filter $R_B(t)$ by parameters built from $p(t)$. Note that while the structures of Fig. 3 and Fig. 4 are equivalent for $p(t) = R_B(t)$, they lose their equivalence for $p(t) \neq R_B(t)$. Another approach, alternative to the two previous ones, is to implement, after the low-pass filtering operation by $p(t)$, the joint ML receiver of the three subcarriers $m = -1, 0, 1$ under a false assumption of temporally white noise. This is equivalent to consider the optimization criterion (7), assuming that $\mathbf{R}_{n,p}(f) = N_0\mathbf{I}$. This approach is justified by the fact that the presence of the filter $R_B(t)$ in the ML structure is directly linked to the noise whitening operation contained in the ML criterion (7). For each of the three sub-optimal receivers previously described, the size of the ISI may be strongly reduced with respect to the one of the ML receiver. Despite this fact, one may still decide to constraint the ISI size used in the Viterbi algorithm, or equivalently the number of states, to have a given size. This will solve the second difficulty and a compromise between performance and complexity must be found. Another option to solve the second difficulty is based on the fact that only two elements of matrix $K_{12}[k]$ are non-zero. This option consists in forcing the decoupling of the metric and to implement two separate receivers for the demodulation of the symbol vectors associated with the odd and even samples time. All these options may be mixed to find the best compromise between performance and complexity. This comparative study of the three sub-optimal receivers jointly with the optimization of the compromise between performance and complexity are out of the scope of this paper and will be analyzed elsewhere.

IV. Conclusion

In this paper, a new Alamouti receiver has been presented to demodulate the OQAM symbols of a FBMC waveform. For each subcarrier, this receiver is based on the ML demodulation of the subcarrier of interest jointly with its two adjacent subcarriers, assuming that the latter are the only ones which overlap. The ML metric has been computed and the structure of the ML receiver has been described. The difficulties to implement this receiver have been pointed out and alternative sub-optimal solutions have been described. The performance analysis of these sub-optimal receivers jointly with the optimization of the compromise between performance and complexity will be analyzed elsewhere.

References

[1] B. Farhang-Boroujeny, "OFDM versus Filter Bank Multicarrier", *IEEE Signal Processing Magazine*, pp. 92-112, May 2011.

[2] G. Wunder, P. Jung, M. Kasparick, T. Wild, F. Schaich, Y. Chen, S. Ten Brink, I. Gaspar, N. Michailow, A. Festag, L. Mendes, N. Cassiau, D. Ktenas, M. Dryjanski, S. Pietrzyk, B. Eged, P. Vago and F. Wiedmann, "5GNOW: Non-Orthogonal Asynchronous Waveforms for Future Mobile Applications", *IEEE Commun. Magazine*, pp. 97-105, Feb. 2014.

[3] B.R. Saltzberg, "Performance of an Efficient Parallel Data Transmission System", *IEEE Trans. Commun. Technol.*, Vol. 15, no. 6, pp. 805-811, Dec. 1967.

[4] B. Hirosaki, "An Orthogonally Multiplexed QAM System using the Discrete Fourier Transform", *IEEE Trans. Commun.*, Vol. 29, no. 7, pp. 982-989, July 1981.

[5] P. Siohan, C. Siclet, N. Lacaille, "Analysis and Design of FBMC/OQAM Systems based on Filterbank Theory", *IEEE Trans. Signal Process.*, Vol. 50, no. 5, pp. 1170-1183, May 2002.

[6] T. Ihalainen, T.H. Stitz, M. Rinne, M. Renfors, "Channel Equalization in Filter Bank based Multicarrier Modulation for Wireless Communications", *Eurasip Journal of applied Signal Process.*, Vol. 2007, Jan. 2007.

[7] D.S. Waldhauser, L.G. Baltar, J. Nossek, "MMSE Subcarrier Equalization for Filter Bank based Multicarrier Systems", *Signal Processing Advances in Wireless Communications (SPAWC)*, pp. 525-529, July 2008.

[8] L.G. Baltar, D.S. Waldhauser, J. Nossek, "MMSE Subchannel Decision Feedback Equalization for Filter Bank based Multicarrier Systems", *IEEE International Symposium in Circuits and Systems (ISCAS)*, pp. 2802-2805, May 2009.

[9] D. Gesbert, M. Shafi, D. Shiu, P. Smith, A. Naguib, "From Theory to Practice: an Overview of MIMO Space-Time Coded Wireless Systems", *IEEE Journal on Selected Areas in Communications*, Vol. 21, no. 3, pp. 281-302, April 2003.

[10] A.J. Paulraj, D.A. Gore, R.U. Nabar, H. Bolcskei, "An Overview of MIMO Communications - A Key to Gigabit Wireless", *Proc. IEEE*, Vol. 92, no. 2, pp. 198-218, Feb. 2004.

[11] M. Caus and A.I. Perez-Neira, "Transmitter-Receiver Designs for Highly Frequency Selective Channels in MIMO FBMC Systems", *IEEE Trans. Signal Process.*, vol. 60, no. 12, pp. 6519-6532, Dec. 2012.

[12] M. Caus and A.I. Perez-Neira, "Multi-Stream Transmission for Highly Frequency-Selective Channels in MIMO-FBMC/OQAM Systems", *IEEE Trans. Signal Process.*, vol. 62, no. 4, pp. 786-796, Feb. 2014.

[13] F. Horlin, J. Fickers, T. Deleu, J. Louveaux, "Interference-Free SDMA for FBMC-OQAM", *Eurasip Journal on Advances in Signal Processing*, 2013, 2013:46.

[14] M. Newinger, L.G. Baltar, A.L. Swindlehurst, J. Nossek, "MISO Broadcasting FBMC System for Highly Frequency Selective Channels", *International Workshop on Smart Antennas (WSA)*, pp. 1-7, March 2014.

[15] Y. Cheng, P. Li, M. Haardt, "Intrinsic Interference Mitigating Coordinated Beamforming for the FBMC/OQAM based Downlink", *Eurasip Journal on Advances in Signal Processing*, 2014, 2014:86.

[16] Y. Cheng, M. Haardt, L.G. Baltar, J.A. Nossek, "Downlink Per-User Multi-Streaming for FBMC/OQAM based Multi-User MIMO with Highly Frequency Selective Channels", *Workshop on Smart Antenna, WSA'15*, Ilmenau (Germany), March 2015.

[17] O.D. Candido, L.G. Baltar, A. Mezghani, J. Nossek, "SIMO/MISO MSE-Duality for Multi-User FBMC with Highly Frequency Selective Channels", *International Workshop on Smart Antennas (WSA)*, pp. 1-7, March 2015.

[18] Y. Cheng, M. Haardt, L.G. Baltar, J.A. Nossek, "Precoder and Equalizer Design for Multi-User MIMO FBMC/OQAM with Highly Frequency Selective Channels", *Proc. ICASSP'15*, Brisbane (Australia), April 2015.

[19] M. El Tabach, J.P. Javaudin, M. Helard, "Spatial Data Multiplexing over OFDM/OQAM Modulations", *Proc. IEEE ICC, ICC'07*, Glasgow, pp. 4201-4206, June 2007.

[20] R. Zakaria, D. Le Ruyet, M. Bellanger, "Maximum Likelihood Detection in Spatial Multiplexing with FBMC", *Proc. European Wireless Conference, EWC'10*, pp. 1038-1041, Apr. 2010.

[21] E. Kofidis, A. Rontogiannis, "Adaptive BLAST Decision-Feedback Equalizer for MIMO FBMC/OQAM Systems", *Proc. IEEE PIMRC, PIMRC'10*, pp. 841-846, Sept. 2010.

[22] T. Ihalainen, A. Ikhlef, J. Louveaux, M. Renfors, "Channel Equalization for Multi-Antenna FBMC/OQAM Receivers", *IEEE Trans. Veh. Technol.*, Vol. 60, no. 5, pp. 2070-2085, 2011.

[23] R. Zakaria, D. Le Ruyet, "A Novel Filter-Bank Multicarrier Scheme to Mitigate the Intrinsic Interference: Application to MIMO Systems", *IEEE Trans. on Wireless Communications*, Vol.11, no.3, pp. 1112-1123, March 2012.

[24] Y. Cheng, M. Haardt, "Widely Linear Processing in MIMO FBMC/OQAM Systems", *Proc. ISWCS'13*, Berlin (Germany), pp. 743-747, Aug. 2013.

[25] S.M. Alamouti, "A Simple Transmit Diversity Technique for Wireless Communications", *IEEE Journ. Sel. Areas Commun.*, Vol. 16, no.18, pp. 1451-1458, 1998.

[26] W.H. Gerstacker, F. Obernosterer, R. Schober, A.T. Lehmann, A. Lampe, P. Gunreben, "Equalization Concepts for Alamouti's Space-Time Block Code", IEEE Trans. On Communications, Vol. 52, no.7, pp. 1178-1190, July 2004.

[27] H. Lin, C. Lele, P. Siohan, "A Pseudo Alamouti Transceiver Design for OFDM/OQAM Modulation with Cyclic Prefix", *SPAWC'09*, pp. 300-304, 2009.

[28] M. Renfors, T. Ihalainen, T.H. Stitz, "A Block-Alamouti Scheme for Filter Bank based Multicarrier Transmission", *Proc. European Wireless Conference, EWC'10*, pp. 1031-1037, Apr. 2010.

[29] C. Lele, P. Siohan, R. Legouable, "The Alamouti Scheme with CDMA-OFDM/OQAM", *Eurasip Journal on Advances in Signal Processing*, Vol. 2010, 13 pages, ID. 703513, 2010.

[30] R. Zakaria, D. Le Ruyet, "On Interference Cancellation in Alamouti Coding Scheme for Filter Bank based Multicarrier Systems", *Proc. ISWCS'13*, pp. 26-30, Berlin, Germany, Aug. 2013.

[31] P. Chevalier, F. Dupuy, "Widely Linear Alamouti Receivers for the Reception of Real-Valued Signals Corrupted by Interferences – The Alamouti SAIC/MAIC Concept", IEEE Trans. On Signal Processing, vol. 59, no.7, pp. 3339-3354, July 2011.

[32] S. Sallem, J.P. Delmas, and P. Chevalier, "Optimal SIMO MLSE Receivers for the Detection of Linear Modulation Corrupted by Non-

circular Interference," *IEEE workshop on Statistical Signal Processing* (SSP'2012), Ann Arbor, USA, Aug. 2012.

[33] G. Ungerboeck, "Adaptive Maximum Likelihood Receiver for Carrier-Modulated Data Transmission Systems", *IEEE Trans. Commun.*, vol. 22, no. 5, pp. 624-636, May 1974.

[34] FP7-ICT PHYDYAS – Physical Layer for Dynamic Spectrum Access and Cognitive Radio, http://www.ict-phydyas.org